Bulgarian Chemical Communications, Volume 50, Special Issue F (pp. 198–204) 2018

Heterogeneous photocatalytic degradation of Reactive Black 5 in aqueous suspension by La-modified ZnO powders

N. Kaneva*, A. Bojinova, K. Papazova, D. Dimitrov

Laboratory of Nanoparticle Science and Technology, Department of General and Inorganic Chemistry, Faculty of Chemistry and Pharmacy, University of Sofia, 1164 Sofia, Bulgaria

Received November 09, 2018; Accepted December 09, 2018

La-modified ZnO powders with different dopants concentration (0, 0.5, 1.0, 1.5, 2.0, 2.5 and 3.0 mol%) are prepared by simple thermal method. The obtained homogeneous charge is annealed at 100 °C. The structural and photocatalytic properties of the samples are characterized by X-ray diffraction, Scanning electron microscopy, BET surface area and UV−vis spectroscopy. The result of XRD shows that La^{3+} is successfully introduced into ZnO lattice. It is found out that the crystallite size of La-modified ZnO is greater as compared to pure ZnO and increases with the increasing La content. Surface area (BET) measurements show higher surface areas and pores volume for La–ZnO catalysts in comparison to pure ZnO. The photocatalytic investigations revealed that all the La-modified ZnO powders exhibited excellent photocatalytic degradation of Reactive Black 5, compared with the ZnO, under UV and visible light irradiation. The optimal dopant concentration is experimentally found to be 2 mol% La in terms of the photocatalytic efficiency. The result shows that La^{3+} doping concentration has a remarkable effect on the efficiency of photocatalytic activity.

Keywords: zinc oxide, lanthanum, Reactive Black 5, photocatalysis.

INTRODUCTION

The annual dye production worldwide is reported as one million tons, 70% of which are azo dyes [1–3]. The azo dyes, containing as chromophore azo group of two nitrogen atoms (–NN–), represent the largest class of textile dyes widely used in the industry. The group of azo dyes includes different types of dyes: reactive, acid, basic, disperse, direct, mordant, metal complex and sulphur dyes. Among these types most used are the reactive azo dyes. At the same time, the reactive azo dyes are also the most problematic pollutants of textile wastewater contaminants, because the reactive dyeing process is accompanied with more than 15% losses of textile dye in wastewater stream [4]. These dyes persist in textile dye house wastewater in concentration range 5–1500 mgl^{-1} due to their poor fixation to fabrics [5]. The purification of dye contaminated wastewaters is quite complicated due to the high chemical, biochemical and photochemical stability of the modern synthetic dyes. Discharge of azo dyes is undesirable not only for aesthetic reasons but also because many azo dyes and their intermediate products are toxic to aquatic life and mutagenic to humans [6, 7]. The conventional physical, biological and chemical methods used for wastewater treatment are not suitable for dye contaminated water.

The physical methods (adsorption, membrane filtration, flocculation, and electrocoagulation) cannot achieve sufficient degradation and mineralization of dyes [8]. These techniques just separate the dye from the water phase and require additional treatment of the generated secondary waste, thus increasing the operation cost [9]. Most of chemical dye removal methods (ozonation [10–12], chlorination [13], wet air oxidation [14, 15], etc.) have essential drawbacks, which limit their application. For example: ozonation and wet air oxidation are efficient, but expensive due to high operation costs, need of special equipment; during chlorination products with higher toxicity compared to the initial compound can be formed. Biodegradation is inefficient for many azo dyes because of their resistance to aerobic degradation and in some cases hazardous aromatic amines are formed [16, 17]. The formed intermediates are more toxic than the dye molecules themselves [6].

An efficient approach for dyes degradation seems the advanced oxidation processes (AOPs) such as

* To whom all correspondence should be sent:
E-mail: nina_k@abv.bg

Fenton reaction and photocatalysis. Fenton's reagent (iron–based catalysts and hydrogen peroxide) is typical powerful oxidizing agent and is explored for organic dye degradation. However, this approach has several limitations: requirement of low pH; sludge residues formation; rapid generation of hydroxyl radicals and their ineffective utilization; limited organic carbon removal [18, 19]. Titania and zinc oxide are the notable and most commonly studied photocatalysts as they are available, chemical stable, low cost, abundance and non-toxic compounds [20]. In the case of ZnO, the lifetime value of electrons is significantly higher and the rate of recombination is lower in comparison with TiO_2, making it an attractive material in photocatalytic applications [21]. Therefore, the trend of publications of nanostructured ZnO photocatalyst in the past decade shows an exponential growth of the investigations in this direction (Fig. 1). Modification of electronic structure via doping is very necessary for improved photocatalytic efficiency. The choice of dopant is of great importance and depends on the desired application. The rare earth elements appear as suitable dopants for photocatalytic applications. Many studies have shown that the doping of semiconductor oxides (ZnO, TiO_2, SnO_2) with RE atoms can improve greatly the photocatalytic performances of these materials [22–24].

In this work, we have selected one of the most used reactive dyes in textile industry – Reactive Black 5 (RB5), as a representative dye contaminant of the industrial wastewaters. RB5 is one of the most common dyes used in the textile industry for dyeing of different fabrics, such as wool, cotton, viscose and polyamide. It is also used in the clinical laboratories as a stain dye for cell biological, hematological and histological tests. The study is a continuation of our previous investigations on: UV induced photodegradation of Malachite Green and Reactive Black 5 by sol-gel obtained ZnO nanoparticles, doped with 0.5 and 1% La [25]; photocatalytic oxidation of ethylene as model air pollutant in gas-phase under UV irradiation by Ln-doped ZnO powders [26]. This study is directed to clarify the influence of dopants concentration on the photocatalytic efficiency and to check the effect in photocatalysis with La-doped ZnO under visible light irradiation.

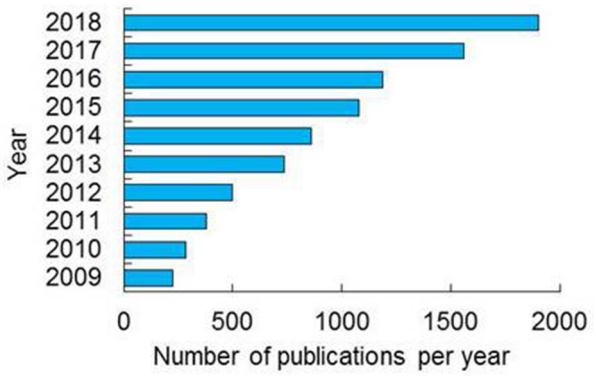

Fig. 1. Rise in the Annual number of publications on photocatalysis with ZnO for the past ten years (2009–2018). Data from Sciencedirect database using the keywords "photocataly*" and "ZnO" in the sections title and article text.

EXPERIMENTAL

Reagents

Commercial oxide powders – ZnO (>99.0%), La_2O_3 (>99.0%) and absolute ethanol, used in the experiments, were purchased from Fluka. Distilled water was used in all experiments.

The organic dye Reactive Black 5 was supplied from Sigma–Aldrich ($C_{26}H_{21}N_5Na_4O_{19}S_6$, molecular weight 991.82, λ_{max} = 595 nm, dye content ca. 55%). This dye was used in the photocatalytic tests as modal water contaminant, due to its huge practical application. RB5 is diazo compound with four phenyl groups. Its water solutions have dark blue color due to connection between aromatic rings and azo groups [27]. RB5 may cause asthma problems, allergy or breathing difficulties, as pointed by the supplier.

Catalysts modification and characterization

Pure ZnO and La-modified powders were obtained by green, simple and fast thermal procedure [26] – at simple preparation conditions, reduced synthesis time, using only stable natural and non-toxic reagents, without any chemical residue after the preparation. La-modified photocatalysts were prepared using commercial oxide powders ZnO and La_2O_3. The calculated amounts of the substances desired ratio (7 series of La-modified ZnO powder samples of 5 g; containing 0, 0.5, 1.0, 1.5, 2.0, 2.5 or 3.0 mol% La respectively) were homogenized in a ceramic vessel with addition of small quantities (8–10 droplets) of ethanol as a mixing medium. The resultant suspension was sonicated for 30 min (IKEDA RIKA ultrasonic bath, 100 V 50/60Hz, 110 W) and then dried for 1 h at 100 °C in order to obtain the ZnO/La powders for photocatalytic tests.

The surface morphology of as-obtained nano-sized powders (pure and La-modified ZnO) was observed by Scanning Electron Microscope (SEM) JSM-5510 (JEOL), operated at 10 kV of accelera-

tion voltage. The investigated samples were coated with gold by JFC-1200 fine coater (JEOL) before observation.

The phase composition and crystallinity of the powder pure and La-modified ZnO samples was identified by X-ray diffraction analysis (XRD) and energy dispersive X-ray (EDX) spectroscopy used for the elemental analysis or chemical characterization of the samples (EDX detector: Quantax 200, Bruker Resolution 126 eV). The XRD was performed at room temperature on powder diffractometer Siemens D500 with CuKα radiation within 2θ range 30–70 at a step of 0.05 2θ and counting time 2 s/step.

The surface area of all powder samples was determined by BET analyses, using standard BET apparatus and volumetric technique. N_2 adsorption and desorption were performed at 77 K. Before the N_2 adsorption the analyzed samples were degassed for 4 h at 150 °C.

The prepared samples were checked for photodegradation of RB5 from aqueous solutions by a standard testing procedure [25]. The volume of dye solution was 250 ml. The catalyst loading was 0.5 $g.L^{-1}$. The initial RB5 concentration was 20 ppm. The irradiation sources were as follows: UVA lamp (Sylvania 18W BLB T8, emitting mainly in the range of 315–400 nm) placed at 10 cm above and linear Tungsram lamp for the visible irradiation (500 W K1R7s 9700 Lm, maximal emission at 700 nm) fixed at 50 cm above the dye solution. The intensity of irradiation at the suspensions surface was: 0.014 W/cm^2 in case of UV light irradiation and 8.9 mW/cm^2 for visible light illumination. Prior testing the suspension was stirred for 30 min in complete darkness to reach the sorption-desorption equilibrium between dye solution and catalysts surface. During the photocatalysis aliquot samples (2 ml) were taken regularly from the investigated solution at selected time intervals. The change in RB 5 concentration with the time of photocatalysis was monitored at 597 nm by UV-VIS spectrophotometer Thermo scientific, Type Evolution 300 BB.

The photocatalytic degradation of RB5 (D%) was calculated by the equation:

$$D\% = (C_0 - C_t)/C_0 \times 100 \quad (1)$$

where C_0 is the initial dye concentration and C_t is the concentration of dye pollutant after selected time of irradiation t.

After measurement, aliquots were returned back to the treated solution. The solutions were stirred constantly by electromagnetic stirrer (rotation speed of 370 rpm). All photocatalytic experiments were performed at room temperature of 23±2 °C.

The pH of the investigated suspensions, determined by pH meter Hanna instruments, was found to be in the range of 5.8–6.1.

RESULTS AND DISCUSSION

X-ray diffraction spectra the analyzed pure and La-modified ZnO powder samples and corresponding EDX analysis are presented in Fig. 2. The EDX results confirm the presence of La at the catalysts surface. The sharp and intense characteristic peaks from the XRD patterns indicate high crystallinity of ZnO. The (100), (002) and (101) peaks of pure ZnO correspond to hexagonal Wurtzite structure type (PDF#77-0191). Any impurity characteristic peaks of phases such as $Zn(OH)_2$ are not observed for all samples. The crystallite size of ZnO, calculated by Scherrer formula from the main peak (101), is about 37 nm for the pure and 42 nm for La-modified ZnO. The XRD spectra of the La-modified ZnO samples (Fig. 2b) are similar to that of pure ZnO. There are very low peaks corresponding to formation of La_2O_3 (PDF # 83-1350), which can be due to the low dopants concentration – 2 mol%. The ZnO crystal structure remains almost unchanged in pure and La-modified samples. The latter indicates also that La is uniformly arranged between the ZnO nanoparticles in form of small clusters La_2O_3.

SEM micrographs shown in Figure 3 compare the microstructure and morphology of pure and ZnO/La (2 mol%) powders. The average particle size of 0.25 μm for ZnO (Fig. 3a and 3b) is determined from the SEM images. As seen from Fig. 3c and 3d, the La-modified ZnO particles are flowerlike in shape. Their average particle size, also determined from SEM micrographs is found to be ~0.43 μm. The SEM images of the rest ZnO/La powders – with La content of 0.5, 1, 1.5, 2.5 and 3 mol% are similar to that of ZnO/La (2 mol%) sample. There is a tendency of slight increasing particle size – from 0.4 to 0.45 μm, with the rise of dopants concentration from 0 to 3 mol%.

Doping of ZnO with La leads to rise of the crystallite size (from 37 to 42 nm) and average particle size (from 0.25 to 0.45 μm) due to the larger ion radius of La^{3+} – 103 pm, than that of Zn^{2+} – 74 pm [28].

The determined specific surface area values according to BET analysis of ZnO and La-modified powder samples are shown in Table 1. The surface area of ZnO/La catalysts is greater than that of pure ZnO (10.30 m^2/g). The surface area values increase with the La concentration up to 0.5, 1, 1.5, there is a maximum at 2 mol% (32.34 m^2/g) and then decrease (2.5 and 3 mol%). Illuminated greater surface area is a key factor for more efficient photocatalysis. The

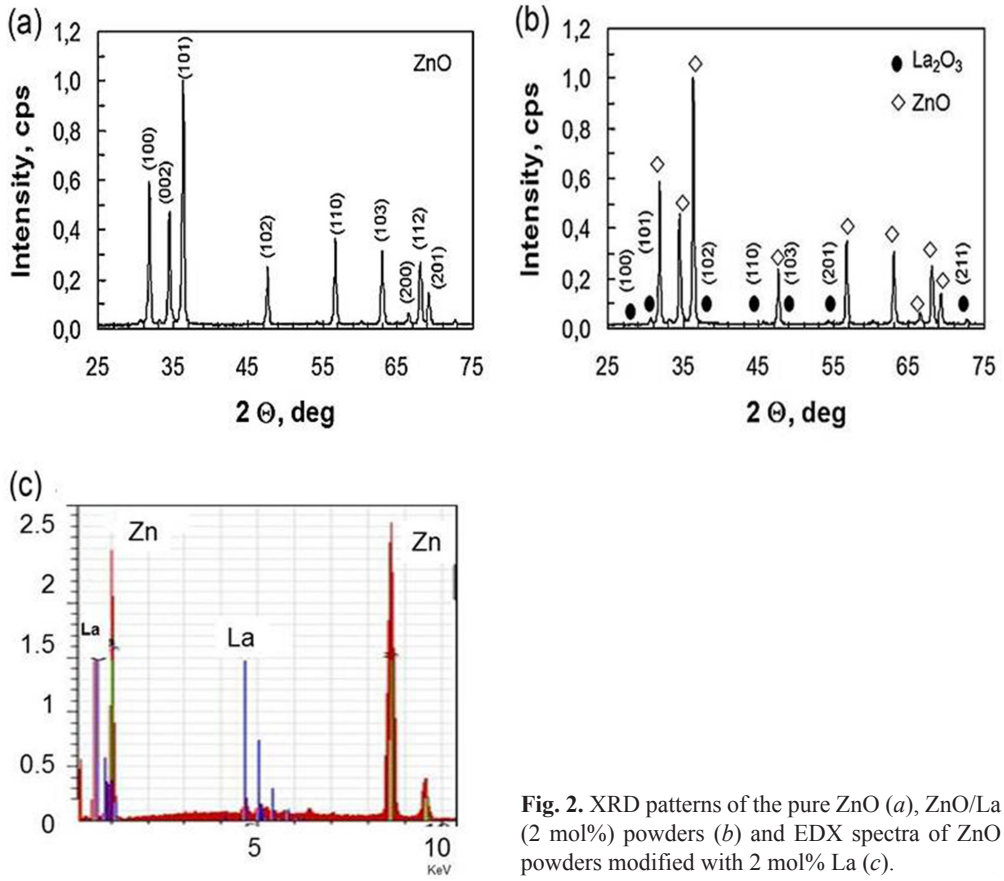

Fig. 2. XRD patterns of the pure ZnO (*a*), ZnO/La (2 mol%) powders (*b*) and EDX spectra of ZnO powders modified with 2 mol% La (*c*).

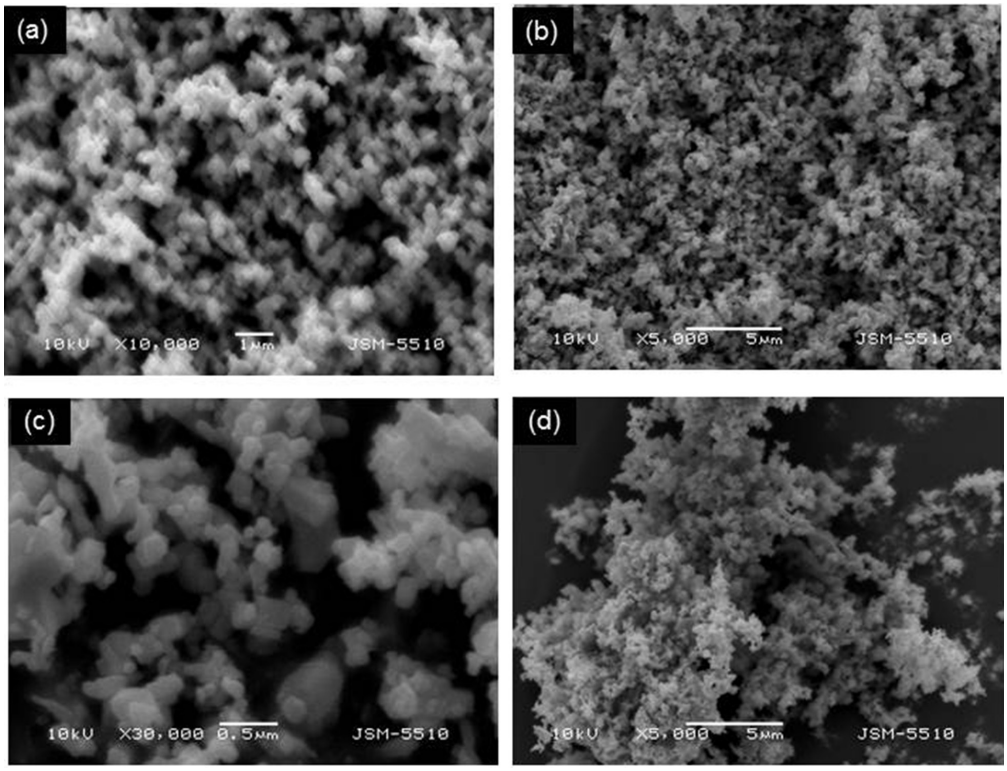

Fig. 3. SEM images of pure (*a*, *b*) and ZnO/La 2 mol% (*c*, *d*) powders at different magnifications.

Table 1. Specific surface area according to BET analysis and photocatalytic results (rate constants, degradation of RB5) of ZnO/La powders

La-doped ZnO samples, mol%	Surface area, m^2/g	Rate constants, min^{-1}		Degradation of Reactive Black 5, %	
		UV	VIS	UV	VIS
0	10.30	0.0431	0.0186	72.35	40.71
0.5	23.68	0.0617	0.0233	84.73	50.22
1.0	25.97	0.0684	0.0282	87.28	54.30
1.5	31.56	0.0725	0.0294	89.71	56.92
2.0	32.34	0.0811	0.0334	92.04	61.86
2.5	30.87	0.0546	0.0194	81.53	46.21
3.0	30.19	0.0524	0.0172	79.31	43.08

effect of this parameter is confirmed in the photocatalytic experiments – the more developed surface increases the total illuminated surface area, thus increasing the number of active surface sites and enhancing the photocatalytic capacity of the samples.

Two series of experiments are performed in order to prove the photocatalytic activity of La-modified ZnO powder catalysts with respect to RB5 degradation. First – the RB5 aqueous suspensions of ZnO/La powders with different dopant concentration (0, 0.5, 1.0, 1.5, 2.0, 2.5 and 3.0 mol%) are exposed to UV light, and second –the experimental tests performed at the same other conditions, but under exposure of visible light illumination. The results from these photocatalytic tests are presented in Figs. 4 and 5. Fig. 4 demonstrates the bleaching kinetics of RB5 aqueous solutions by all kinds of La-modified ZnO powder catalysts exposed to UV (Fig. 4a) and visible (Fig. 4b) light irradiation. As seen from the presented data, the pure ZnO shows the lowest photcatalytic efficiency, as compared to that of La-modified samples, irrespective or type of illumination. The best photocatalytic performance is manifested by the sample ZnO/La (2 mol%) in both cases – under UV and under visible light irradiation. The heterogeneous photocatalytic process is considered to be pseudo-first-order reaction with respect to RB5 and can be described according to the equation:

$$\ln(C_t/C_0) = -kt \qquad (2)$$

Here C_0 is the initial concentration of dye solution, C_t is the dye concentration at reaction time t, and k is the rate constant of photocatalysis. The rate constants can also be calculated from the plots of $\ln(C_0/C)$ versus reaction time presented in Fig. 4. The initial slope of the linear fit of the experimental data by Eq (2) (the solid lines in the figure) gives the

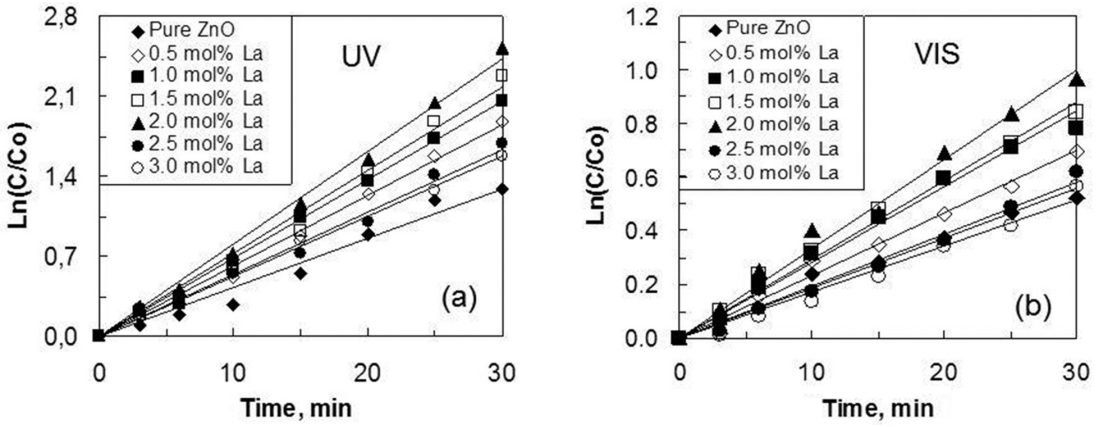

Fig. 4. Kinetics of RB5 dye photodecomposition from 20 ppm aqueous solutions by ZnO and different La-modified ZnO powder catalysts under UV (*a*) and visible (*b*) light illumination. The catalysts concentration is 1 g/dm^3.

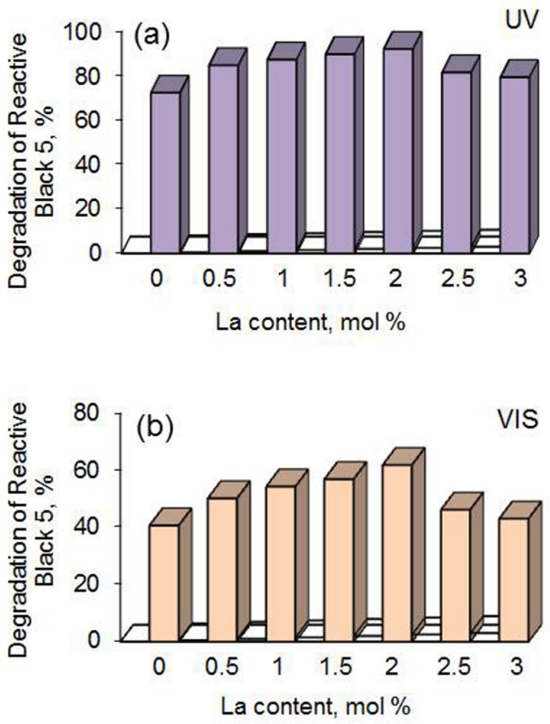

Fig. 5. Photomineralization degree of Reactive Black 5, depending on dopants concentration of La-modified ZnO powders. The data correspond to 30 min illumination time with UV (*a*) and visible light (*b*).

rate constant value, *k*. The values of as-calculated rate constants are presented in Table 1.

A comparison of the achieved degree of photocatalytic mineralization of RB5 in 20 ppm water suspension by all powder samples at 30 min of irradiation is shown in Fig. 5. According to the presented data, the order of photodegradation degree of doped ZnO powders is as follows: 0<0.5<1<1.5<2>2.5>3 mol% La. Moreover, according to Table 1 where the relationship between different parameters are clearly seen, it should be pointed that this order is the same as that of surface area and rate constant values of photocatalysis.

The above results demonstrated that there are certain relationships between doping and photocatalytic activity. The photocatalytic efficiency at first increased with La concentration, reaches maximum and then decreases. The higher activity of La-modified samples can be attributed to production of high number surface oxygen vacancies and defects (related to the different charge and electronegativity of La and Zn ions and also geometrical reasons). La^{3+} easily attracts O atoms from the ZnO lattice, as it is more positive and has larger ion radius. As higher number of oxygen vacancies is, as stronger is the adsorption of OH^- ions onto the ZnO surface, namely, the larger content of oxygen vacancies and defects, the higher photocatalytic activity. During the process of photocatalytic reactions, oxygen vacancies and defects could become the centers to capture photoinduced electrons so that the recombination of photoinduced electrons and holes could be effectively inhibited. In addition – the introduced by doping La energy levels, lead to enhanced photocatalytic efficiency of ZnO, due to suppressed recombination of the photogenerated electrons and holes [30].

At concentrations, higher than the optimal of La doping, the photocatalytic efficiency decreases. The reason is that a lot of chemical bonds Zn–O–La between the three elements occur and that is why the content of surface oxygen vacancies and surface defects decreases [29].

The results show that La-modified ZnO powders are promising and efficient catalysts for textile wastewater purification.

CONCLUSIONS

La-modified ZnO powders are prepared by simple hydrothermal method. Their photocatalytic efficiency has been established in Reactive Black 5 mineralization from aqueous suspensions under UV and visible light irradiation. Doping of ZnO with La leads to rise of the crystallite size (XRD) and average particle size (SEM) due to the larger ion radius of La^{3+}. Surface area (BET) measurements show higher surface areas for La–modified ZnO catalysts in comparison to pure ZnO. The optimal dopant concentration is established – 2 mol% La. The results show that La^{3+} doping has a remarkable effect on the photocatalytic efficiency of zinc oxide photocatalysts, dye to formation of surface oxygen vacancies and defects and successful charge separation.

Acknowledgements: *Authors are grateful to Operational program "Science and Education for Smart Growth", project BG05M2OP001-2.009-0028, DFNI-T02/16, Russian Presidential Program of engineer advanced trading and Horizon 2020 project ID: 692146-H2020-eu.4.b "Materials Networking".*

REFERENCES

1. M. Stoyanova, I. Slavova, St. Christoskova, V. Ivanova, *Appl. Cat. A*, **476**, 121 (2014).
2. S. Garcia-Segura, F. Centellas, C. Arias, J. A. Garrido, R. M. Rodriguez, P. L. Cabot, E. Brillas, *Electrochim. Acta*, **58**, 303 (2011).
3. B. Palas, G. Ersoz, S. Atalay, *Chemosphere*, **209**, 823 (2018).

4. M. S. Lucas, J. A. Peres, *Dyes and Pigments*, **71**, (3) 236 (2006).
5. J. Pierce, *J. Soc. Dyers Colourists*, **110**, 131 (1994).
6. S. Meric, D. Kaptan, T. Olmez, *Chemosphere*, **54**, 435 (2004).
7. A. Gottlieb, C. Shaw, A. Smith, A. Wheatley, S. Forsyth, *J. Biotechnol.*, **101**, 49 (2003).
8. F. Harrelkas, A. Azizi, A. Yaacoubi, A. Benhammou, M.N. Pons, *Desalination*, **235**, 330 (2009).
9. T. Robinson, G. McMullan, R. Marchant, P. Nigam, *Bioresour. Technol.*, **77**, 247 (2001).
10. M. Constapel, M. Schellanträger, J.M. Marzinkowski, S. Gäb, *Water Res.*, **43**, 733 (2009).
11. S. Song, H. Ying, Z. He, J. Chen, *Chemosphere*, **66**, 1782 (2007).
12. F. Zhang, A. Yediler, X. Liang, *Chemosphere*, **67**, 712 (2007).
13. Q. Zeng, J. Fu, Y. Shi, H. Zhu, *Ozone Sci. Eng*., **31**, 37 (2009).
14. B. Gözmen, B. Kayan, A.M. Gizir, A. Hesenov, *J. Hazard. Mater.*, **168**, 129 (2009).
15. L. Lei, Q. Dai, M. Zhou, X. Zhang, *Chemosphere*, **68**, 1135 (2007).
16. W. Azmi, R. K. Sani, U. C. Banerjee, *Enzyme Microb. Technol.*, **22**, 185 (1998).
17. J. Ge, J. Qu, *Appl. Catal. B*, **47**, 133 (2004).
18. F. Ji, Ch. Li, L. Deng, *Chem. Eng. J.*, **178**, 239 (2011).
19. R. M. Liu, S. H. Chen, M. Y. Hung, C. S. Hsu, J. Y. Lai, *Chemosphere*, **59**, 117 (2005).
20. J. Fanga, H. Fana, Y. Ma, Z. Wang, C. Qi, *Appl. Surf. Sci.*, **332**, 47 (2015).
21. M. A. Hernández-Carrillo, R. Torres-Ricárdez, M. F. García-Mendoza, E. Ramírez-Morales, G. Pérez-Hernández, *Catalysis Today*, in press (2018). Available online 30 April 2018 https://doi.org/10.1016/j.cattod.2018.04.060.
22. H. V. Fajardo, E. Longo, L. F. D. Probst, A. Valentini, N. L. V. Carreño, M. R. Nunes, A. P. Maciel, E. R. Leite, *Nanoscale Res. Lett.*, **3**, 194 (2008).
23. S. Anandan, Y. Ikuma, V. Murugesan, *Int. J. Photoenergy*, **2012**, (2012) Article 921412.
24. F. Jiang, Z. Peng, Y. Zang, X. Fu, *J. Adv. Ceram.*, **2**, (3) 201 (2013).
25. N. Kaneva, A. Bojinova, K. Papazova, *J. Phys. Conf. Ser.*, **682**, 012022 (2016).
26. N. Kaneva, A. Bojinova, K. Papazova, D, Dimitrov, A. Eliyas, *Bulg. Chem. Commun.*, **49**, (G) 172 (2017).
27. N. Yousefi, A. Fatehizadeh, E. Azizi, M. Ahmadian, A. Ahmadi, A. Rajabizadeh, A. Toolabi Sacha, *J. Environ. Studies*, **1**, 81 (2011).
28. A. F. Wells, Structural Inorganic Chemistry, 5th ed., Clarendon Press, Oxford, 1984, p. 1288.
29. J. Liqiang, S. Xiaojun, X. Baifu, W. Baiqi, C. Weimin, F. Hongganga, *J. Solid State. Chem.*, **177**, (10) 3375 (2004).
30. N. Kaneva, A. Bojinova, K. Papazova, D, Dimitrov, *Catalysis Today*, **252**, 113 (2015).